Flexural-Torsional Bifurcations of a Cantilever Beam Under Potential And Circulatory Forces: Part I Nonlinear Model and Stability Analysis

Achille Paolone, Marcello Vasta, Angelo Luongo

Flexural-torsional bifurcations of a cantilever beam under potential and circulatory forces I. Non-linear model and stability analysis

Achille Paolone[a,*], Marcello Vasta[b], Angelo Luongo[c]

[a]*DISEG, University of Rome "La Sapienza", via Eudossiana 18, 00184 Rome, Italy*
[b]*PRICOS, University of Chieti-Pescara "G.D'Annunzio", viale Pindaro 42, 65127 Pescara, Italy*
[c]*DISAT, University of L'Aquila, 67040 Monteluco di Roio, L'Aquila, Italy*

Abstract

The stability of a cantilever elastic beam with rectangular cross-section under the action of a follower tangential force and a bending conservative couple at the free end is analyzed. The beam is herein modeled as a non-linear Cosserat rod model. Non-linear, partial integro-differential equations of motion are derived expanded up to cubic terms in the transversal displacement and torsional angle of the beam. The linear stability of the trivial equilibrium is studied, revealing the existence of buckling, flutter and double-zero critical points. Interaction between conservative and non-conservative loads with respect to the stability problem is discussed. The critical spectral properties are derived and the corresponding critical eigenspace is evaluated.

Keywords: Buckling; Flutter; Double-zero bifurcation; Cosserat rod model; Stability analysis; Non-conservative loads

1. Introduction

Thin-walled beams are commonly utilized in civil and aeronautical industry. As well known, the structures exhibit a flexural-torsional Eulerian buckling when subjected to conservative forces. However, different critical behaviors arise if non-conservative loads (e.g. follower forces) are applied, such as those caused by the thrust of rocket and jet engines, dry friction in automotive disk and drum-brake systems. Under these circumstances the loss of stability may happen either by divergence or by flutter, depending on the mechanical properties of the structure. In addition, when conservative and non-conservative loads are applied, simultaneously the critical boundaries, in the control parameters space, show an interaction phenomenon [1]. Namely, the critical conservative load increases in presence of non-conservative forces, while the critical non-conservative load decreases in presence of conservative forces. Several reviews of problems involving non-conservative forces have been published [2,3], as well as books on this subject, [4–7]. To understand the very complex problem arising in real structures due to the interactions between circulatory and potential forces, several academic problems have been studied, such as Beck's, Reut's, Leipholz's columns and their generalizations. These works are mainly confined to the linear stability analysis from which the destabilizing effects of the damping as well as the stabilizing effects of the follower forces on the conservative forces are examined [8]. However, the attention has been mainly focused on the linear stability analysis and very little over the postcritical behavior. Recently the authors devoted particular attention to the study of multiple dynamic bifurcation points for discrete systems [9].

In this paper the non-linear analysis of the so-called generalized Beck's column is performed. In Part I of the paper, the stability of a fixed-end elastic beam with rectangular cross-section under the action of a follower tangential force and a bending conservative couple at the free end is analyzed. The beam model herein considered is the non-linear Cosserat rod model [10–13], where four internal kinematic constraint are introduced. These conditions allow to derive the non-linear equations of motions in terms of two displacements only. In particular, non-linear partial integro-differential equations of motion are derived,

* Corresponding author. Tel.: +39 06 44585193; fax: +39 06 488 4852.
E-mail address: achille.paolone@uniroma1.it (A. Paolone).

Nomenclature

A	cross-section area
b	beam height cross-section
$\mathscr{C}_0$	beam reference configuration
$\mathscr{C}_t$	actual beam configuration
c_v, c_ϑ	flexural and torsional damping coefficients
E	Youngs modulus
F	intensity of the conservative forces
F_0	prestress intensity of the conservative forces
G	tangential elastic modulus
h	beam length cross-section
I_G	polar inertia
I_x, I_y	flexural inertia momentum
J	torsional inertia
l	beam length
(M_x, M_y), M_t	flexural and torsional components of the dynamic contact couple
p, m	non-dimensional control parameters
P	intensity of the follower force
P_0	prestress intensity of the follower force
(T_x, T_y), N	shear and axial components of the dynamic contact force
u, v, w	displacement components
ε_z	axial strain
φ_x, φ_y, ϑ	elementary rotations
γ_x, γ_y	shear deformations
(κ_x, κ_y), κ_t	bending and torsional curvatures
ω_v, ω_ϑ	natural flexural and torsional frequencies
ρ	mass density
ζ_v, ζ_ϑ	non-dimensional flexural and rotational damping coefficients
$\mathbf{a}_i$	fixed initial reference frame ($i = 1, 2, 3$)
$\mathbf{b}$	density external force
$\mathbf{c}$	density external couple
$\mathbf{D}_i$	orthonormal directors ($i = x, y, z$) of the beam in reference configuration
$\mathbf{d}_i$	orthonormal directors ($i = x, y, z$) of the beam in actual configuration
$\mathbf{e}$	strain vectors
$\mathbf{K}$	curvature tensor
$\mathbf{m}$	internal contact couple
$\mathbf{m}_0$	prestress static contact couple
$\tilde{\mathbf{m}}$	dynamic contact couple
$\mathbf{R}$	orthogonal rotation tensor
$\mathbf{t}$	internal contact force
$\mathbf{t}_0$	prestress static contact force
$\tilde{\mathbf{t}}$	dynamic contact force
$\mathbf{u}$	displacement vector
$\mathbf{x}$	actual position vector
$\mathbf{X}$	reference position vector

expanded up to cubic terms, in terms of the transversal displacement and the torsional angle of the beam. The linear stability of the trivial equilibrium is first studied. It reveals the existence of buckling, flutter and double-zero (DZ) critical points. Interaction between conservative and non-conservative loads with respect to the stability problem is discussed and the spectral properties are analyzed.

In Part II of the paper the non-linear partial integro-differential equations and the boundary conditions are recast in first-order form. The critical properties of the adjoint problem are studied; in particular the generalized Keldysh eigenfunctions are obtained at the double-zero bifurcation point. The postcritical behavior is finally analyzed through a perturbation method around simple buckling (divergence bifurcation), simple flutter (Hopf bifurcation) and DZ critical points (Takens–Bogdanova–Arnold bifurcation).

2. Model

The case under study consists of a straight fixed-end beam subjected to a *non-conservative follower force* of intensity P_0 and a *conservative couple* at the free end made of *two conservative forces* of intensity F_0, collinear to the beam axis and applied at the H and K points (Fig. 1a). The beam is assumed sufficiently slender in order to neglect the axial and shear deformations (Kirchhoff's beam); moreover a narrow rectangular cross-section is considered ($b \ll h$) (Fig. 1a), so that the flexural stiffness around the axis orthogonal to the plane's couple can be assumed infinitely higher than the other stiffness. It follows that the straight reference configuration is an equilibrium state for each values of the loads parameters (P_0, F_0). The adopted beam model is an internally constrained one-dimensional Cosserat rod [10–12].

2.1. Kinematic analysis

A Lagrangian description of the motion is adopted (Fig. 1b). The beam is assumed to be straight in its rest reference configuration $\mathscr{C}_0$, coincident with the prestressed equilibrium state, with directors $\mathbf{D}_j$ ($j = x, y, z$), oriented as the orthonormal versors of a fixed inertial reference frame $(O; \mathbf{a}_j)$. The reference configuration is therefore described by $\mathbf{X}(s) = s\mathbf{a}_z$, with $s \in (0, l)$ and l being the beam length. The actual beam configuration $\mathscr{C}_t$ at time t is specified by the vector displacement $\mathbf{u}(s, t)$ and the position vector $\mathbf{x}(s, t)$, connected by $\mathbf{x}(s, t) = \mathbf{X}(s) + \mathbf{u}(s, t)$, and by the proper orthogonal tensor $\mathbf{R}(s, t)$ describing the rotation of the actual directors $\mathbf{d}_j = \mathbf{R}\mathbf{D}_j$.

The beam strain measures are defined as the following *strain vectors* and *curvature tensor*, respectively [12]:

$$\mathbf{e} := \mathbf{R}^\mathrm{T}\mathbf{x}' - \mathbf{X}', \quad \mathbf{K} = \mathbf{R}^\mathrm{T}\mathbf{R}', \tag{1}$$

where a prime denotes differentiation with respect to s. Denoting by (u, v, w) the components of $\mathbf{u}$ in the fixed inertial reference $(O; \mathbf{a}_j)$ and decomposing the rotation group $\mathbf{R}$ into

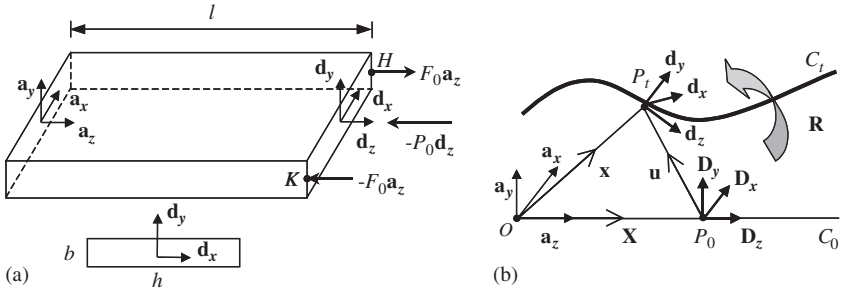

Fig. 1. (a) Beam model and (b) kinematic description.

the product of three successive elementary rotations of amplitude, respectively, φ_x, φ_y, ϑ, the components in the reference configuration of the elongation vector $\mathbf{e}$ are

$$\gamma_x = (\cos\varphi_y\cos\vartheta)u' + (\sin\varphi_x\sin\varphi_y\cos\vartheta + \cos\varphi_x\sin\vartheta)v' + (\sin\varphi_x\sin\vartheta - \cos\varphi_x\sin\varphi_y\cos\vartheta)w' + 2\sin\varphi_x\sin\vartheta - \cos\varphi_x\sin\varphi_y\cos\vartheta, \tag{2}$$

$$\gamma_y = -(\cos\varphi_y\sin\vartheta)u' + (\cos\varphi_x\cos\vartheta - \sin\varphi_x\sin\varphi_y\sin\vartheta)v' + (\sin\varphi_x\cos\vartheta + \cos\varphi_x\sin\varphi_y\sin\vartheta)w' + \sin\varphi_x\cos\vartheta + \cos\varphi_x\sin\varphi_y\sin\vartheta, \tag{3}$$

$$\varepsilon_z = (\sin\varphi_y)u' - (\sin\varphi_x\cos\varphi_y)v' + (\cos\varphi_x\cos\varphi_y)w' + \cos\varphi_x\cos\varphi_y - 1, \tag{4}$$

where γ_x, γ_y are the *shear deformations* while ε_z is the *axial strain*. The components of the axial vector associated with the curvature tensor $\mathbf{K}$ are

$$\begin{aligned}\kappa_x &= \varphi_y'\sin\vartheta + \varphi_x'\cos\varphi_y\cos\vartheta,\\ \kappa_y &= \varphi_y'\cos\vartheta - \varphi_x'\sin\vartheta\cos\varphi_y,\\ \kappa_t &= \vartheta' + \varphi_x'\sin\varphi_y,\end{aligned} \tag{5}$$

where κ_x, κ_y are the *bending curvatures* and κ_t the *torsional curvature*. Since the beam is slender and with high flexural stiffness around the principal axis $\mathbf{d}_y$, when compared with the flexural stiffness around $\mathbf{d}_x$, four internal constraints are introduced, namely $\gamma_x = \gamma_y = \varepsilon_z = \kappa_y = 0$. These conditions constitute a set of four coupled non-linear differential equations, in six kinematic variables (u, v, w, φ_x, φ_y, ϑ), allowing hence for the description of the actual configuration in terms of two kinematic variables only. Assuming v and ϑ as independent variables, by means of a standard perturbative procedure, the following asymptotic expansion, truncated at the third order, are obtained (see Appendix A):

$$u = -\int_0^s\int_0^s \vartheta v''\,\mathrm{d}s\,\mathrm{d}s, \quad w = -\int_0^s \frac{1}{2}v'^2\,\mathrm{d}s,$$

$$\varphi_x = -v' - \frac{1}{6}v'^3, \quad \varphi_y = -\int_0^s \vartheta v''\,\mathrm{d}s, \tag{6}$$

where the geometrical boundary conditions

$$\mathbf{u}(0,t) = \mathbf{0} \quad \mathbf{R}(0,t) = \mathbf{I} \tag{7}$$

have been used. Furthermore, the non-zero curvature measures becomes

$$\kappa_x = -v'' - \frac{1}{2}(v'^2v'' + \vartheta^2v''), \quad \kappa_t = \vartheta' + v''\int_0^s \vartheta v''\,\mathrm{d}s. \tag{8}$$

2.2. Equations of motion

Denoting by $\mathbf{t}(s,t)$ and $\mathbf{m}(s,t)$ the internal contact force and couple, respectively, and with $\mathbf{b}(s,t)$ and $\mathbf{c}(s,t)$ the density external forces and couples, respectively, representing damping and inertial actions, the dynamic balance equations are

$$\mathbf{t}' + \mathbf{b} = \mathbf{0}, \quad \mathbf{m}' + \mathbf{x}' \times \mathbf{t} + \mathbf{c} = \mathbf{0}, \tag{9}$$

where $\mathbf{x}' = \mathbf{X}' + \mathbf{u}' = \mathbf{a}_z + \mathbf{u}'$. By considering different damping coefficients for the translational and rotational viscous forces (c_v, c_ϑ), and neglecting the rotational viscous and inertial forces around the principal cross-section (x, y) axes, the following expressions hold in Eq. (9):

$$\mathbf{b} = -\rho A\ddot{\mathbf{u}} - c_v\dot{\mathbf{u}}, \quad \mathbf{c} = -(\rho I_G\ddot{\vartheta} + c_\vartheta\dot{\vartheta})\mathbf{d}_z, \tag{10}$$

where ρ, A, I_G, are the mass density, the cross-section area and the polar inertia, respectively. The external loads, applied at the free end, consist of a follower force, $\mathbf{P} = -P_0\mathbf{d}_z$, and a conservative couple made of two forces applied in H, K (Fig. 1a), $\mathbf{F}_{H,K} = \pm F_0\mathbf{a}_z$, statically equivalent to a torque $\mathbf{M} = F_0h\,\mathbf{d}_x \times \mathbf{a}_z$. Henceforth, the equilibrium boundary conditions are

$$\mathbf{t}(l,t) = -P_0\mathbf{d}_z, \quad \mathbf{m}(l,t) = M_0\mathbf{d}_x \times \mathbf{D}_z, \tag{11}$$

where $M_0 = F_0h$, h being the length of the beam cross-section along the $\mathbf{d}_x$ director.

The prestresses contact force and couple are obtained solving Eqs. (9) and (11) with $\mathbf{x}' = \mathbf{D}_z$, obtaining

$$\mathbf{t}_0(s) = -P_0\mathbf{D}_z, \quad \mathbf{m}_0(s) = -M_0\mathbf{D}_y. \tag{12}$$

Decomposing the contact force and couple ($\mathbf{t}$, $\mathbf{m}$) into the sum of prestress static ($\mathbf{t}_0$, $\mathbf{m}_0$) and dynamic ($\tilde{\mathbf{t}}$, $\tilde{\mathbf{m}}$) components and taking into account the prestress solution (Eq. (12)), equilibrium field Eq. (9) for the dynamic components are (omitting tilde):

$$\mathbf{t}' + \mathbf{b} = \mathbf{0}, \quad \mathbf{m}' + \mathbf{D}_z \times \mathbf{t} + \mathbf{u}' \times (\mathbf{t}_0 + \mathbf{t}) + \mathbf{c} = \mathbf{0} \tag{13}$$

while the boundary conditions Eq. (11) becomes

$$\mathbf{t}(l,t) = P_0(\mathbf{D}_z - \mathbf{d}_z), \quad \mathbf{m}(l,t) = M_0(\mathbf{D}_y + \mathbf{d}_x \times \mathbf{D}_z). \tag{14}$$

The introduction of inner constraints implies the presence of reactive terms in contact actions. Thus, the contact actions in the actual basis $(\mathbf{x}; \mathbf{d}_j)$, namely $\mathbf{t} = T_x\mathbf{d}_x + T_y\mathbf{d}_y + N\mathbf{d}_z$ and $\mathbf{m} = M_x\mathbf{d}_x + M_y\mathbf{d}_y + M_t\mathbf{d}_z$, are decomposable in an active part (M_x, M_t) related to non-null deformations (κ_x, κ_t), and a reactive part ($\mathbf{t}$, M_y) associated with null deformations ($\mathbf{e}$, κ_y). The active part is related to displacements via a constitutive law

$$M_x = EI\kappa_x, \quad M_t = GJ\kappa_t, \tag{15}$$

where I is the weak inertia momentum ($I = I_x$), J the torsional inertia, E the Young modulus, and G the tangential elastic modulus. The reactive part is condensed via direct integration of the equations of motion. From Eq. $(13)_1$ the reactive contact force $\mathbf{t}$ is derived, namely

$$\mathbf{t} = P_0(\mathbf{D}_z - \mathbf{d}_z) - \int_l^s \mathbf{b}\,\mathrm{d}s, \tag{16}$$

where the boundary conditions Eq. (14) have been used. By introducing the following non-dimensional quantities:

$$\hat{t} = \omega_v t, \quad \hat{s} = \frac{s}{l}, \quad \hat{v} = \frac{v}{l}, \quad \omega_v^2 = \frac{EI}{\rho A l^4}, \quad \omega_\vartheta^2 = \frac{GJ}{\rho I_G l^2},$$
$$\alpha = \frac{\omega_\vartheta}{\omega_v},$$
$$p = \frac{P_0 l^2}{EI}, \quad m = \frac{M_0 l}{EI}, \quad \xi^2 = \frac{Al^2}{I_G}, \quad \zeta_v = \frac{c_v}{2\omega_v \rho A},$$
$$\zeta_\vartheta = \frac{c_\vartheta}{2\omega_\vartheta \rho I_G}, \tag{17}$$

the components of the reactive contact force in the actual basis, omitting the hat, are

$$t_x = -p\int_0^1 v''\vartheta\,\mathrm{d}s - \int_1^s\int_0^s\int_0^s [(\vartheta v'')^{\cdot\cdot} + 2\zeta_v(\vartheta v'')^{\cdot}]\,\mathrm{d}s\,\mathrm{d}s\,\mathrm{d}s,$$
$$t_y = -pv'(1) + \int_1^s (\ddot{v} + 2\zeta_v\dot{v})\,\mathrm{d}s,$$
$$t_z = p\frac{v'(1)^2}{2} - \frac{1}{2}\int_1^s\int_0^s [(v'^2)^{\cdot\cdot} + 2\zeta_v(v'^2)^{\cdot}]\,\mathrm{d}s\,\mathrm{d}s, \tag{18}$$

where $t_j = T_j l^2/EI$ $(j = x, y, z)$ and the approximated kinematic field Eq. (6) have been used (see Eq. (A.5) in Appendix A for the expression of tensor $\mathbf{R}$).

The moment balance dynamic equations Eq. $(13)_2$, with the associated boundary conditions Eq. $(14)_2$, projected along the $\mathbf{a}_y$ direction, allows for the evaluation of the reactive moment $M_y(s)$. By a perturbative analysis, we have (see Appendix B)

$$\begin{aligned} m_y(s) = &-\frac{m}{2}v'(1)^2 + v''(1)\vartheta(1) - \frac{\alpha^2}{\xi^2}\vartheta'(1)v'(1) \\ &- \int_1^s \left[\frac{\alpha^2}{\xi^2}(\vartheta' v')' - (v''\vartheta)'\right]\mathrm{d}s - \int_1^s t_x\,\mathrm{d}s \\ &- m\int_1^s (v'v'' + \vartheta\vartheta')\,\mathrm{d}s + p\int_0^s\int_1^s \vartheta v''\,\mathrm{d}s\,\mathrm{d}s \end{aligned} \tag{19}$$

having set $m_y = M_y l/EI$, where Eqs. (6) and (8) have also been used. The non-dimensional non-linear equations of motion are derived by projecting the moment balance dynamic equations Eq. $(13)_2$ along the $\mathbf{a}_x$, $\mathbf{a}_z$ directions:

$$\begin{aligned} &\ddot{v} + 2\zeta_v\dot{v} + v^{\mathrm{IV}} - m\vartheta'' + pv'' + n_v(v,\vartheta) = 0, \\ &\ddot{\vartheta} + 2\alpha\zeta_\vartheta\dot{\vartheta} - \alpha^2\vartheta'' - \xi^2 m v'' + n_\vartheta(v,\vartheta) = 0, \end{aligned} \tag{20}$$

where

$$\begin{aligned} n_v(v,\vartheta) = &(m_y\vartheta)'' - \frac{1}{2}(t_y v'^2)' - (t_z v')' \\ &+ \frac{\alpha^2}{\xi^2}\left(\vartheta\vartheta' v''' + \vartheta'^2 v'' - \vartheta'''\int_0^s v''\vartheta\,\mathrm{d}s\right) \\ &+ \left(v''^3 + 3v'v''v''' + \frac{v'^2 v^{\mathrm{IV}}}{2}\right) \\ &+ m\left(\vartheta'^2\vartheta + \frac{\vartheta''\vartheta^2}{2} - 2v''^2\vartheta - 2v'''\int_0^s v''\vartheta\,\mathrm{d}s\right), \end{aligned} \tag{21}$$

$$\begin{aligned} n_\vartheta(v,\vartheta) = &(m_y v')' + t_x v' + t_y\int_0^s v''\vartheta\,\mathrm{d}s \\ &- \xi^2\left(v'v''\vartheta' + v'v'''\vartheta + v'''\int_0^s v''\vartheta\,\mathrm{d}s\right) \\ &- \alpha^2\left(v''^2\vartheta - \frac{\vartheta'' v'^2}{2} - v'v''\vartheta' + v'''\int_0^s v''\vartheta\,\mathrm{d}s\right) \\ &- m\xi^2\left(\frac{\vartheta^2 v''}{2} - v'\vartheta\vartheta' - \vartheta'\int_0^s v''\vartheta\,\mathrm{d}s\right). \end{aligned} \tag{22}$$

The associated kinematic boundary conditions (Eq. (7)) are

$$v = 0, \;\; v' = 0, \;\; \vartheta = 0 \quad \text{in } s = 0 \tag{23}$$

while the mechanical boundary conditions (Eq. $(14)_2$), projected along the $\mathbf{a}_x$, $\mathbf{a}_z$ directions are

$$\begin{aligned} &\alpha^2\vartheta' + \xi^2 m v' + b_t(v,\vartheta) = 0, \\ &-v''' + m\vartheta' + b_T(v,\vartheta) = 0 \quad \text{in } s = 1, \\ &v'' + b_M(v,\vartheta) = 0, \end{aligned} \tag{24}$$

where

$$\begin{aligned} b_t(v,\vartheta) = &-\xi^2 m_y v' + [(\alpha^2 + \xi^2)v'' - \xi^2 m\vartheta]\int_0^1 v''\vartheta\,\mathrm{d}s \\ &+ \xi^2 v''v'\vartheta - \frac{\alpha^2}{2}v'^2\vartheta' - \frac{\xi^2 m}{2}v'\vartheta^2, \\ b_T(v,\vartheta) = &-(m_y\vartheta)' + \frac{\alpha^2}{\xi^2}\left(-\vartheta\vartheta' v'' + \vartheta''\int_0^1 v''\vartheta\,\mathrm{d}s\right) \\ &- \frac{m}{2}\vartheta^2\vartheta' - \left(v'v''^2 + \frac{v'^2 v'''}{2}\right) \\ &+ \frac{p}{2}v'^3 + 2mv''\int_0^1 v''\vartheta\,\mathrm{d}s, \\ b_M(v,\vartheta) = &\, m_y\vartheta - \left(\frac{\alpha^2}{\xi^2}\vartheta' + mv'\right)\int_0^1 v''\vartheta\,\mathrm{d}s \\ &+ \frac{1}{2}v'^2 v'' - \frac{m}{2}v'^2\vartheta. \end{aligned} \tag{25}$$

3. Stability analysis of the trivial path

In this section, the buckling and flutter boundaries are derived by means of static and dynamic approach, respectively. The non-dimensional loads p and m (Eq. (17)) are assumed as control parameters.

3.1. Buckling

As well known, for the evaluation of the critical buckling boundaries, it is sufficient to consider only the *linear static* parts of Eqs. (20), (23) and (24). By eliminating the torsional angle ϑ, the following ordinary differential equation in terms of the v variable only is obtained:

$$v^{\mathrm{IV}} + \eta^2(p,m)v'' = 0, \tag{26}$$

where

$$\eta^2(p,m) = p + \frac{\xi^2 m^2}{\alpha^2} \tag{27}$$

with the condensed boundary conditions

$$\begin{aligned} &v = 0,\ \ v' = 0 \quad \text{in } s = 0,\\ &v'' = 0,\ \ v''' + \eta^2(0,m)v' = 0 \quad \text{in } s = 1. \end{aligned} \tag{28}$$

Solution of Eq. (26) returns

$$\phi_v(s) = c_0 + c_1 s + c_2 \sin \eta s + c_3 \cos \eta s \tag{29}$$

while the torsional angle $\vartheta(s)$ is given by

$$\phi_\vartheta(s) = -\frac{\xi^2 m}{\alpha^2}\phi_v(s) \tag{30}$$

having set $\phi_v = v$, $\phi_\vartheta = \vartheta$. Inserting Eq. (29) into the boundary conditions Eq. (28), a homogeneous linear system for the c_k's ($k = 0, 1, 2, 3$), is obtained, resulting in a transcendental real characteristic equation

$$f_s(p,m) = \cos[\eta(p,m)] - 1 + \frac{\eta^2(p,m)}{\eta^2(0,m)} = 0. \tag{31}$$

Eq. (31) implicitly define the buckling boundaries in the load parameters space (p, m). They consist of an infinity of branches, each originating in the m-axis, reaching a maximum in the first quadrant and then closing again in the m-axis. The intersection of these curves on the m-axis supply the critical flexural-torsional buckling moments, whose values can be explicitly evaluated from Eq. (31) taking $p = 0$, obtaining (see e.g. [14])

$$m_j = (1 + 2j)\frac{\pi\alpha}{2\xi}, \quad j = 0, 1, \ldots \tag{32}$$

Figs. 2a and b show the buckling boundaries scenario, for a steel beam with $\omega_v = 0.013$, $\omega_\vartheta = 1.445$ and $\xi = 86.550$, in the normalized load parameters space $(p^* = p/p_0, m^* = m/m_0)$, where p_0 is the non-dimensional follower Beck's critical load, equal to $p_0 = 20.19$ and m_0 is the critical flexural-torsional buckling moment, obtained by Eq. (32) for $j = 0$. Figs. 3 shows the flexural and torsional components of buckling eigenmodes defined in Eqs. (29) and (30) evaluated at point B on the first buckling curve, Fig. 2b. The first critical boundary confirms the known results previously obtained by other authors (see, e.g. [8]) about the stabilizing effects of non-conservative forces in buckling phenomena caused by conservative forces, since p increases the lowest critical couple m_0.

3.2. Flutter

The evaluation of the flutter boundaries requires the analysis of the small oscillations around the trivial configuration, ruled by non-dimensional *linearized* equation of motion obtained by Eq. (20), with the associated *kinematic* boundary conditions, Eq. (23), and the *mechanical* boundary conditions, Eq. (24). Flutter occurs when the linear motion $v(s,t) = \phi_v(s)\exp \lambda t$, $\vartheta(s,t) = \phi_\vartheta(s)\exp \lambda t$, is harmonic, i.e. the eigenvalue λ is purely imaginary, $\lambda = \mathrm{i}\omega$, where ω

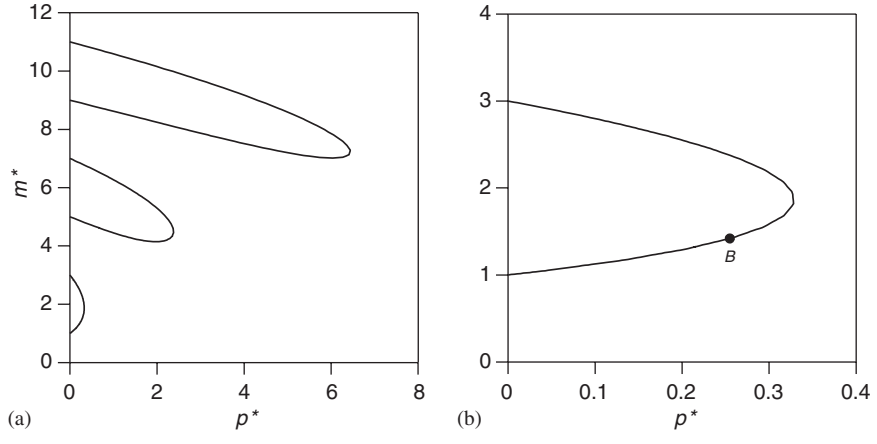

Fig. 2. (a) Buckling boundaries scenario and (b) first buckling curve.

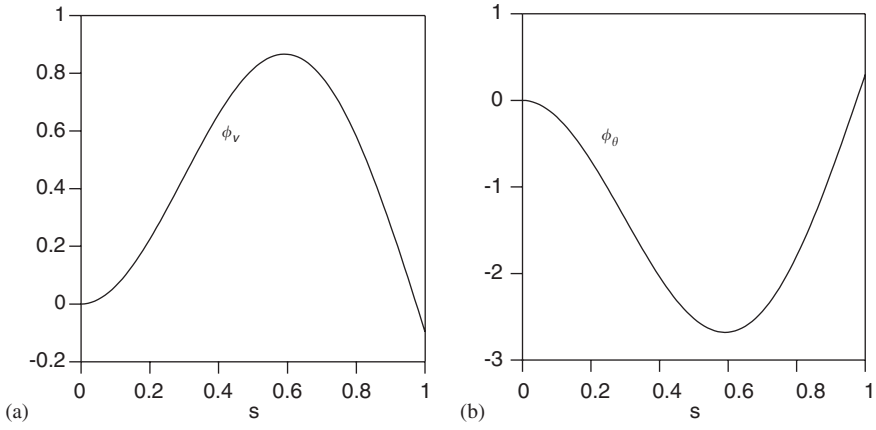

Fig. 3. Buckling eigenmodes: (a) transversal and (b) torsional.

is the non-dimensional linearized small oscillation frequency. The associated solution reads

$$\begin{bmatrix} v \\ \vartheta \end{bmatrix} = \sum_{j=1}^{6} C_j \begin{bmatrix} a_j \\ b_j \end{bmatrix} e^{\beta_j s} e^{i\omega t}, \tag{33}$$

where

$$a_j = -\omega^2 + 2i\alpha\zeta_\vartheta\omega - \alpha^2\beta_j^2, \quad b_j = \xi^2\beta_j^2 m. \tag{34}$$

Moreover, C_j are complex unknown coefficients and β_j are the space frequencies, roots of the characteristic equation

$$\beta^6 + \gamma_1\beta^4 + \gamma_2\beta^2 + \gamma_3 = 0, \tag{35}$$

where

$$\begin{aligned} \gamma_1 &= [p\alpha^2 - \xi^2 m^2 + 2i\alpha\zeta_\vartheta\omega + \omega^2]/\alpha^2, \\ \gamma_2 &= -i[2(\zeta_v\alpha^2 + p\alpha\zeta_\vartheta) + i(p - \alpha^2)\omega]\omega/\alpha^2, \\ \gamma_3 &= [4\zeta_v\zeta_\vartheta\alpha + 2i(\zeta_v + \alpha\zeta_\vartheta)\omega - \omega^2]\omega^2/\alpha^2. \end{aligned} \tag{36}$$

By imposing that solution Eq. (33) respects the associated boundary conditions, a critical condition of the form

$$f_d(p, m, \omega) = 0 \tag{37}$$

is obtained, where $f_d(p, m, \omega)$ is a complex function of the control parameters (p, m) and of the frequency ω. Eq. (37) implicitly define the flutter boundaries in the (p, m) plane. Since closed-form solutions for Eq. (37) are not available, a path-following procedure has been used instead. The frequency parameter ω has been adopted as continuation parameter, the space frequencies β_j then evaluated by numerically solving Eq. (35), and finally the (p, m) parameters obtained zeroing the real and imaginary parts of $f_d(p, m, \omega)$. The origin of the flutter curves on the p-axis supply the critical follower loads, that for $\zeta = 0$ coincide with the Beck's critical values [8]. These can be explicitly evaluated as solution of the transcendental equation

$$\tan\sqrt{p} = \sqrt{p} \tag{38}$$

whose first solutions are $p_1 = 20.19$, $p_2 = 59.68$, $p_3 = 118.89$. In the normalized parameters space (p^*, m^*) the flutter curves for the beam under examination are shown in Fig. 4a, for different values of the damping parameters $\zeta = \zeta_v = \zeta_\vartheta$. The flutter boundaries confirm that the conservative action m has a non-stabilizing effect on flutter critical axial load p. Moreover, as shown in Fig. 4a, the flutter boundaries tend to a unique point, DZ, not depending by the damping values (similarly to the Herrmann model [2]), belonging to the first buckling critical boundary, in correspondence of which the natural frequency ω goes to zero. Fig. 4b show this circumstance: the natural frequency ω evaluated along the flutter curves, parameterized in m, attains a zero value corresponding to the *DZ* point and increases while approaching the p-axis. Figs. 5a and b show the flexural and torsional flutter eigenmodes defined in Eq. (33) at the *F* point of Fig. 4a.

3.3. Double zero

It is well known [15] that the coalescent point of a buckling and a flutter boundaries identifies a DZ critical point, where the characteristic equation (Eq. (37)) admits the zero natural frequency with multiplicity equal to two. Although the DZ point belong to the buckling curve, a static approach does not permit its evaluation because of its intrinsic dynamic nature. The evaluation of this point can be pursued independent of Flutter analysis, by considering the McLaurin series expansion of the dynamic characteristic equation Eq. (37) [16]:

$$f_d(p, m, \omega) = f_0(p, m) + f_1(p, m)\omega + O(\omega^2), \tag{39}$$

where

$$f_0(p, m) = f_s(p, m), \quad f_1(p, m) = \left.\frac{\partial f_d(p, m, \omega)}{\partial\omega}\right|_{\omega=0} \tag{40}$$

and by imposing that

$$f_0(p, m) = 0, \quad f_1(p, m) = 0. \tag{41}$$

Eq. (41) confirms analytically the dynamic nature of the DZ point, because of its dependency on the damping parameters $(\zeta_v, \zeta_\vartheta)$. In contrast it does not depend on the inertial terms, since these are of higher order near the zero frequency. Fig. 6

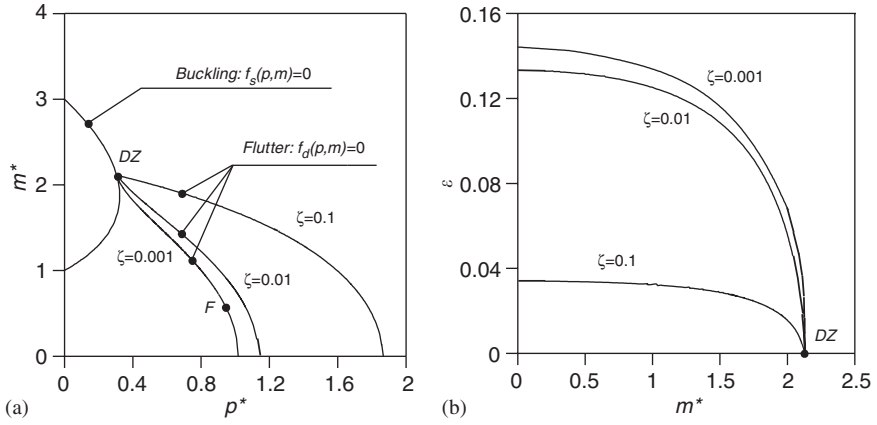

Fig. 4. (a) Buckling and flutter boundaries and (b) critical frequency along the flutter curves.

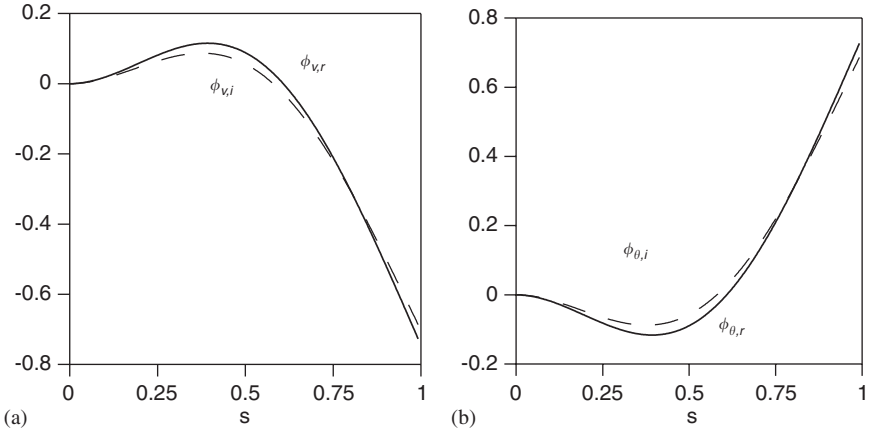

Fig. 5. Flutter eigenmodes, real and imaginary components: (a) transversal and (b) torsional.

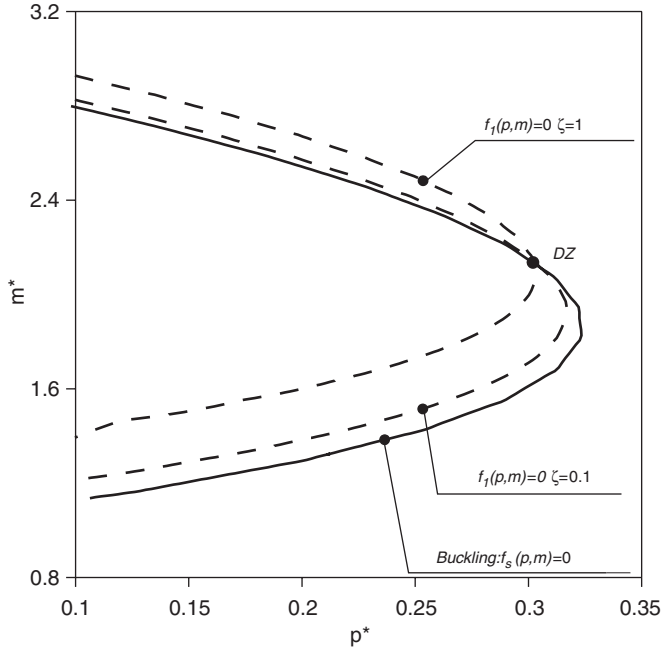

Fig. 6. Double-zero (DZ) point as intersection of buckling boundary (solid line) and zero-gradient conditions (dashed line).

shows the buckling boundary (solid line, Eq. $(41)_1$), and the zero-gradient condition (dashed line, Eq. $(41)_2$), for different values of the damping parameter ζ. These curves cross the buckling curve at the DZ point, allowing its evaluation.

It is worth noting that to the algebraic multiplicity two of the zero frequency corresponds a geometric multiplicity equal to one, i.e. only one proper eigenfunction, coincident with the buckling mode, exists. To complete the basis of the eigenfunctions a Keldish chain must be considered, examined in detail in Part II.

4. Conclusions

The stability of narrow rectangular cross-section beams with thin walls under simultaneous action of conservative and non-conservative loads has been discussed. The beam has been considered as a one-dimensional continuum model with a local rigid structure, capable of describing the mechanical behavior of the body in finite displacement regime. Non-linear, partial integro-differential equations of motion have been derived expanded up to cubic terms in the transversal displacement and torsional angle of the beam. The linear stability of the trivial equilibrium reveals the existence of buckling, flutter and DZ

critical points. The structure exhibits three instability forms, two of codimension one (buckling and flutter) and one of codimension two (double-zero bifurcation). The spectral properties and critical modes of these three instability mechanism have been derived and discussed.

Appendix A. Perturbation analysis of the kinematic constraints

The (v, ϑ) components are assumed as active kinematic variables while the remaining $(u, w, \varphi_x, \varphi_y)$ as passive variables, following from the internal constraints $\gamma_x = \gamma_y = \varepsilon = \kappa_y = 0$.

$$\mathbf{R} = \begin{bmatrix} 1 - \dfrac{\vartheta^2}{2} & -\vartheta + \dfrac{\vartheta^3}{6} & \int_0^s v''\vartheta\,\mathrm{d}s \\ \vartheta - v'\int_0^s v''\vartheta\,\mathrm{d}s - \dfrac{v'^2\vartheta}{2} - \dfrac{\vartheta^3}{6} & 1 - \dfrac{\vartheta^2}{2} - \dfrac{v'^2}{2} & v' \\ -\int_0^s v''\vartheta\,\mathrm{d}s - v'\vartheta & -v' + \vartheta\int_0^s v''\vartheta\,\mathrm{d}s + \dfrac{v'\vartheta^2}{2} & 1 - \dfrac{v'^2}{2} \end{bmatrix}. \tag{A.5}$$

To solve them, a perturbation parameter ε is introduced by scaling the active variables as $v = \varepsilon\hat{v}$, $\vartheta = \varepsilon\hat{\vartheta}$. An inspection of Eqs. (2)–(4), expanded in ε series, reveals that φ_x is an odd function of ε, while u, w and φ_y are even functions of ε. Therefore, expanding these variables in Taylor series, it follows that

$$\begin{pmatrix} u \\ w \\ \varphi_y \end{pmatrix} = \varepsilon^2 \begin{pmatrix} u_2 \\ w_2 \\ \varphi_{y_2} \end{pmatrix} + \mathrm{O}(\varepsilon^4),$$
$$\varphi_x = \varepsilon\varphi_{x_1} + \varepsilon^3\varphi_{x_3} + \mathrm{O}(\varepsilon^5). \tag{A.1}$$

By substituting Eq. (A.1) in the constraint equations, expanding them up to ε^3-order terms and separately equating to zero terms with the same power of ε, the following perturbation equations are drawn:

$$\begin{aligned}
&\varepsilon: \quad \varphi_{x_1} = -v' \\
&\varepsilon^2: \quad \begin{cases} u_2' - \varphi_{y_2} = -v'\vartheta - \vartheta\varphi_{x_1}, \\ w_2' \;\; = \varphi_{x_1}v' + \frac{1}{2}\varphi_{x_1}^2, \\ \varphi_{y_2} = \vartheta\varphi_{x_1}', \end{cases} \\
&\varepsilon^3: \quad \varphi_{x_3} = -w_2'\varphi_{x_1} + \vartheta u_2' + \tfrac{1}{2}v'\vartheta^2 \\
&\qquad\qquad -\varphi_{y_2}\vartheta + \tfrac{1}{2}v'\varphi_{x_1}^2 + \tfrac{1}{6}\varphi_{x_1}^3 + \tfrac{1}{2}\vartheta^2\varphi_{x_1},
\end{aligned} \tag{A.2}$$

where the hat has been omitted on v and ϑ. In a similar way, the geometrical boundary conditions are obtained from Eq. (7):

$$\begin{aligned}
&\varepsilon: \quad \varphi_{x_1}(0) = 0, \\
&\varepsilon^2: \quad u_2(0) = w_2(0) = \varphi_{y_2}(0) = 0, \\
&\varepsilon^3: \quad \varphi_{x_3}(0) = 0.
\end{aligned} \tag{A.3}$$

Eqs. (A.2) and (A.3) must be solved for the unknown coefficients of series (A.1) and given known terms v and ϑ. By solving them in chain, we have

$$\begin{aligned}
&\varepsilon: \quad \varphi_{x_1} = -v', \\
&\varepsilon^2: \quad u_2 = -\int_0^s\int_0^s \vartheta v''\,\mathrm{d}s\,\mathrm{d}s, \quad w_2 = -\int_0^s \frac{v'^2}{2}\,\mathrm{d}s, \\
&\qquad\qquad u_2 = -\int_0^s \vartheta v''\,\mathrm{d}s, \\
&\varepsilon^3: \quad \varphi_{x_3} = -\frac{v'^3}{6}.
\end{aligned} \tag{A.4}$$

By substituting relationships Eq. (A.4) in Eq. (A.1) and reabsorbing the perturbation parameter ε, Eq. (6) are finally found. With Eq. (A.4), the non-zero curvatures κ_x, κ_t, expanded up to ε^3-order, reads as in Eq. (8). Furthermore, the rotation tensor $\mathbf{R}$ becomes

Appendix B. Perturbation analysis of the equilibrium equation

The moment balance equation Eq. $(13)_2$ is considered; in it

$$\begin{aligned}
\mathbf{m}' = {} & M_x'\mathbf{d}_x + M_y'\mathbf{d}_y + M_t'\mathbf{d}_z + M_x k_t\mathbf{d}_y + M_y(k_x\mathbf{d}_z \\
& - k_t\mathbf{d}_x) - M_t k_x\mathbf{d}_y,
\end{aligned} \tag{B.1}$$

where use has been made of $\mathbf{d}_j' = \mathbf{R}\mathbf{K}\mathbf{D}_j$ and $k_y = 0$. Projecting on the $(\mathbf{a}_x, \mathbf{a}_y, \mathbf{a}_z)$ basis, the following scalar equations are derived:

$$\begin{aligned}
&M_x' r_{xx} + M_y' r_{yx} + M_t' r_{zx} + M_x k_t r_{yx} + M_y(-k_t r_{xx} + k_x r_{zx}) \\
&\quad - M_t k_x r_{yx} - T_y(1 + w') + v'(T_z - P_0) = 0, \\
&M_x' r_{xy} + M_y' r_{yy} + M_t' r_{zy} + M_x k_t r_{yy} + M_y(-k_t r_{xy} + k_x r_{zy}) \\
&\quad - M_t k_x r_{yy} + T_x(1 + w') - u'(T_z - P_0) = 0, \\
&M_x' r_{xz} + M_y' r_{yz} + M_t' r_{zz} + M_x k_t r_{yz} + M_y(-k_t r_{xz} + k_x r_{zz}) \\
&\quad - M_t k_x r_{yz} + u' T_y - v' T_x = 0,
\end{aligned} \tag{B.2}$$

where $r_{ij} = \mathbf{D}_i \cdot \mathbf{d}_j$ $(i, j = x, y, z)$ are the elements of the rotation tensor $\mathbf{R}$. Similarly, the projected associated boundary conditions Eq. $(14)_2$ writes

$$\begin{aligned}
&M_x r_{xx} + M_y r_{yx} + M_t r_{zx} + M_0 r_{xy} = 0, \\
&M_x r_{xy} + M_y r_{yy} + M_t r_{zy} + M_0(1 - r_{xx}) = 0, \\
&M_x r_{xz} + M_y r_{yz} + M_t r_{zz} = 0.
\end{aligned} \tag{B.3}$$

The constitutive law Eq. (15) and the kinematic relations Eqs. (6) and (8) are then used to express the active moments M_x and M_t in terms of displacements (v, ϑ) and moreover the asymptotic form Eq. (A.5) of the rotation tensor $\mathbf{R}$ is used. Field equation Eq. $(B.2)_2$ with the associate boundary condition Eq. $(B.3)_2$ is asymptotically solved for the unknown reactive moment M_y.

By introducing the scaling $M_y = \varepsilon^2 \hat{M}_y$, $v = \varepsilon \hat{v}$, $\vartheta = \varepsilon \hat{\vartheta}$, these reads

$$
\begin{aligned}
&M_y' + GJ(\vartheta' v'' + \vartheta'' v') - EI(v''' \vartheta + v'' \vartheta') \\
&\quad + M_0(\vartheta' \vartheta + v'' v') - P_0 \int_0^s \vartheta v'' \, \mathrm{d}s + T_x = 0, \\
&M_y + GJ \vartheta' v' - EI v'' \vartheta + \frac{M_0}{2} v'^2 = 0, \quad s = l,
\end{aligned} \tag{B.4}
$$

where terms up to the ε^2 order have been considered and the hat omitted. After integration, solution Eq. (18) is recovered. The remaining Eq. $(B.2)_{1,3}$ and boundary Eq. $(B.3)_{1,3}$, after differentiation lead to the final equations Eq. (20).

References

[1] M.A. Langthjem, Y. Sugiyama, Dynamic stability of columns subjected to follower loads: a survey, J. Sound Vib. 238 (5) (2000) 809–851.

[2] G. Herrmann, Stability of equilibrium of elastic systems subjected to nonconservative forces, Appl. Mech. Rev. 20 (1967) 103–108.

[3] C. Sundararaian, The vibration and stability of elastic systems subjected to follower forces, Shock Vib. Dig. 7 (1975) 89–105.

[4] Y.G. Panovko, I.I. Gubanova, Stability and Oscillations of Elastic Systems, Consultants Bureau, New York, 1965.

[5] H. Ziegler, Principles of Structural Stability, Blaisdell, Waltham, MA, 1968.

[6] H. Leipholz, Stability of Elastic Systems, Sijthoff and Noordhoff, Alphen aan den Rijn, 1980.

[7] Z.P. Bazant, L. Cedolin, Stability of Structures, Oxford University Press, Oxford, 1991.

[8] V.V. Bolotin, Non-conservative Problems of the Theory of Elastic Stability, Pergamon Press, Oxford, 1963.

[9] A. Luongo, A. Di Egidio, A. Paolone, Multiple scale bifurcation analysis for finite-dimensional autonomous systems, Recent Research Developments in Sound and Vibration, vol. 1, Transworld Research Network, Kerala, India, 2002, pp. 161–201.

[10] P. Villaggio, Mathematical Models for Elastic Structures, Cambridge University Press, Cambridge, 1997.

[11] S.S. Antman, Nonlinear Problems of Elasticity, Springer, New York, 1995.

[12] G. Capriz, A contribution to the theory of rods, Riv. Mat. Univ. Parma 7 (4) (1981).

[13] N. Rizzi, A. Tatone, Nonstandard models for thin-walled beams with a view to applications, J. Appl. Mech. 63 (1996) 399–403.

[14] S.G. Timoshenko, J.M. Gere, Theory of Elastic Stability, McGraw-Hill, New York, 1961.

[15] A. Luongo, A. Paolone, A. Di Egidio, Sensitivities and linear stability analysis around a double zero eigenvalue, AIAA J. 38 (4) (2000) 702–710.

[16] A. Luongo, A. Paolone, M. Vasta, On the characterization of multiple bifurcation points of mechanical systems driven by conservative and non conservative loads (in Italian), XVI National Congress AIMETA, Ferrara, 2003.